On-Line Monitoring Imidacloprid and Thiacloprid in Celery Juice Using Quartz Crystal Microbalance

ARTICLE *in* ANALYTICAL CHEMISTRY · JANUARY 2009

Impact Factor: 5.64 · DOI: 10.1021/ac801786a · Source: PubMed

2 AUTHORS, INCLUDING:

Xinyan bi
Singapore Institute for Clinical Sciences
26 PUBLICATIONS **449** CITATIONS

Anal. Chem. **2009,** *81,* 527–532

Articles

On-Line Monitoring Imidacloprid and Thiacloprid in Celery Juice Using Quartz Crystal Microbalance

Xinyan Bi and Kun-Lin Yang*

Department of Chemical and Biomolecular Engineering, National University of Singapore, 4 Engineering Drive 4, Singapore 117576

In this article, we report a quartz crystal microbalance (QCM)-based detection method which allows the identification and quantification of two neonicotinoid pesticides, imidacloprid and thiacloprid, in aqueous solutions and celery juice. To achieve high selectivity, molecular imprinted monolayers (MIMs), which can either recognize 1 μM of imidacloprid or 1 μM of thiacloprid, are prepared from alkanethiols self-assembled on QCM sensor chips with preadsorbed templates (either imidacloprid or thiacloprid). Our experimental results show that the detection limit can be improved by using alkanethiols having longer hydrocarbon chains. For example, MIMs prepared from hexadecanethiol have dissociation constants 2−5 times smaller than those prepared from octanethiol. To detect two neonicotinoids in vegetable samples simultaneously, we also develop a new type of MIM with two different templates. A single QCM decorated with this MIM can respond to 10 μM of imidacloprid and 10 μM thiacloprid in celery juice in a real-time manner.

Neonicotinoids, such as imidacloprid, thiacloprid, and acetamiprid, are a new class of pesticides against a variety of insects.[1,2] Unlike traditional pesticides such as organophosphates or carbamates, most neonicotinoid pesticides contain a chloronicotinyl moiety, which has high agonistic affinity for nicotinic acetylcholine receptors found in many insects.[3−6] Despite of their specific toxicity for insects and high effectiveness, neonicotinoid residues are still harmful to human beings. For example, maximum allowable thiacloprid residues in European Union (EU) range from 0.5 to 1 mg/kg for some fruiting vegetables.[7] Therefore, a suitable method for analyzing neonicotinoid residues in the concentration ranges relevant to the EU standard is needed.[8] In the past, gas chromatography/mass spectroscopy (GC/MS) has been used to analyze neonicotinoid residues found in vegetable or soil samples.[9−11] On the other hand, for detecting neonicotinoids such as imidacloprid and thiacloprid, liquid chromatography/mass spectroscopy (LC/MS) is more suitable because of their low volatility.[12−15] However, both GC/MS and LC/MS require large and expensive instrumentations and cannot be used for on-line monitoring of neonicotinoids in water or vegetable samples.

Applications of quartz crystal microbalances (QCMs) for various chemical and biological sensing applications have been demonstrated in the past.[16−23] To obtain high selectivity for analytes of interest, a sensitive layer which can recognize target molecules needs to be coated on the QCM surface. For example, sensitive layers containing acetylcholinesterase (AChE) have been used to detect organophosphorous and carbamate pesticides.[24,25]

* To whom correspondence should be addressed. E-mail: cheyk@nus.edu.sg. Phone: +65-6516-6614.

(1) Ferrer, I.; Thurman, E. M.; Fernández-Alba, A. R. F. *Anal. Chem.* **2005**, *77*, 2818–2825.
(2) Tomizawa, M.; Talley, T. T.; Maltby, D.; Durkin, K. A.; Medzihradszky, K. F.; Burlingame, A. L.; Taylor, P.; Casida, J. E. *Proc. Natl. Acad. Sci. U.S.A.* **2007**, *104*, 9075–9080.
(3) Bai, D.; Lummis, S. C. R.; Leicht, W.; Breer, H.; Sattelle, D. B. *Pestic. Sci.* **1991**, *33*, 197–204.
(4) Nauen, R.; Ebbinghaus-Kintscher, U.; Schmuck, R. *Pest Manage. Sci.* **2001**, *57*, 577–586.
(5) Liu, M. Y.; Casida, J. E. *Pestic. Biochem. Physiol.* **1993**, *46*, 200–206.
(6) Liu, M. Y.; Casida, J. E. *Pestic. Biochem. Physiol.* **1993**, *46*, 40–46.
(7) http://eur-lex.europa.eu/LexUriServ/site/en/oj/2007/l_329/l_32920071214en00400051.pdf (accessed August 15, 2008).
(8) Pous, X.; Ruíz, M. J.; Picó, Y.; Font, G.; Fresenius, J. *Anal. Chem.* **2001**, *371*, 182–189.
(9) Uroz, F. J.; Arrebola, F. J.; Egea-Gonzalez, F. J.; Martinez-Vidal, J. L. *Analyst* **2001**, *126*, 1355–1358.
(10) Vilchez, J. L.; El-Khattabi, R.; Fernandez, J.; Gonzalez-Casado, A.; Navalon, A. *J. Chromatogr. A* **1996**, *746*, 289–294.
(11) Navalon, A.; Gonzalez-Casado, A.; El-Khattabi, R.; Vilchez, J. L.; Fernandez-Alba, A. R. *Analyst* **1997**, *122*, 579–581.
(12) Fernandez-Alba, A. R.; Valverde, A.; Aguera, A.; Contreras, M.; Chiron, S. *J. Chromatogr. A* **1996**, *721*, 97–105.
(13) Ruiz de Erenchun, N.; Gomez de Balugera, Z.; Goicolea, M. A.; Barrio, R. J. *Anal. Chim. Acta* **1997**, *349*, 199–206.
(14) Garrido-Frenich, A.; Egea-Gonzalez, F. J.; Martinez-Vidal, J. L.; Parrilla-Vazquez, P.; Mateu-Sanchez, M. *J. Chromatogr. A* **2000**, *869*, 497–504.
(15) Martinez-Galera, M.; Garrido-Frenich, A.; Martinez-Vidal, J. L.; Parrilla-Vazquez, P. *J. Chromatogr. A* **1998**, *799*, 149–154.
(16) Lieberzeit, P. A.; Dickert, F. L. *Anal. Bioanal. Chem.* **2007**, *387*, 237–247.
(17) Zeng, H.; Jiang, Y.; Xie, G.; Yu, J. *Sens. Actuators B* **2007**, *122*, 1–6.
(18) McCallum, J. J. *Analyst* **1989**, *114*, 259–272.
(19) Nishino, H.; Nihira, T.; Mori, T.; Okahata, Y. *J. Am. Chem. Soc.* **2004**, *126*, 2264–2265.
(20) Nishino, H.; Murakawa, A.; Mori, T.; Okahata, Y. *J. Am. Chem. Soc.* **2004**, *126*, 14752–14757.
(21) Manaka, Y.; Kudo, Y.; Yoshimine, H.; Kawasaki, T.; Kajikawa, K.; Okahata, Y. *Chem. Commun.* **2007**, 3574–3576.
(22) Ward, M. D.; Buttry, D. A. *Science* **1990**, *249*, 1000–1007.
(23) Buttry, D. A.; Ward, M. D. *Chem. Rev.* **1992**, *92*, 1355–1379.
(24) Abad, J. M.; Pariente, F.; Hernández, L.; Abruña, H. D.; Lorenzo, E. *Anal. Chem.* **1998**, *70*, 2848–2855.

10.1021/ac801786a CCC: $40.75 © 2009 American Chemical Society
Published on Web 12/16/2008

Because the detection principle of this method is based on the inhibitory mechanism, it is not very useful for distinguishing two or more closely related neonicotinoids. Another method of preparing sensitive layer is based on three-dimensional (3D) molecular imprinting techniques in which monomers are polymerized around target analytes (templates) and form recognition sites for binding target molecules.[26−31] For example, Lieberzeit et al. used the 3D molecular imprinting technique to prepare QCM sensors for detecting small aromatics, polycyclic aromatic hydrocarbons, and parapox virus ovis. They found that the selectivity obtained from this technique allows one to differentiate two similar molecules which only differ in one methyl group.[32] However, one limitation of the 3D molecularly imprinted polymer is the slow response time because target molecules need to diffuse to recognition sites embedded deep inside the polymer. To overcome this problem, a two-dimensional (2D) molecularly imprinting method has been proposed recently. In this method, organosilanes or thiols are self-assembled on solid surfaces in the presence of templates.[33−38] After the removal of the templates, the resulting cavities formed in the self-assembled monolayers (SAMs) can be used to readsorb template molecules. However, competitive bindings between thiols (or organosilanes) and templates during the 2D imprinting process limit the number of surface imprinted sites. To address this issue, Husson and Li[39] proposed a two-step method for preparing 2D molecularly imprinted monolayers (MIMs) on gold surfaces. In this method, gold surfaces with preadsorbed templates were exposed to 2-mercaptoethanol vapors which self-assembled around the templates. However, it is not clear whether MIMs prepared following Husson's method can be used to distinguish neonicotinoids with very similar structures.

Herein, we investigate the feasibility of using MIMs-decorated QCM for detecting and differentiating two closely related neonicotinoids, imidacloprid and thiacloprid. Detection limits and cross-sensitivity obtained from imidacloprid-imprinted and thiacloprid-imprinted monolayers were studied and compared. Because the effect of thicknesses of the 2D MIMs on the detection limit and selectivity has not been reported before, we also prepared different MIMs by using alkanethiols with different chain lengths and compared the binding of neonicotinoids to these MIMs. Finally,

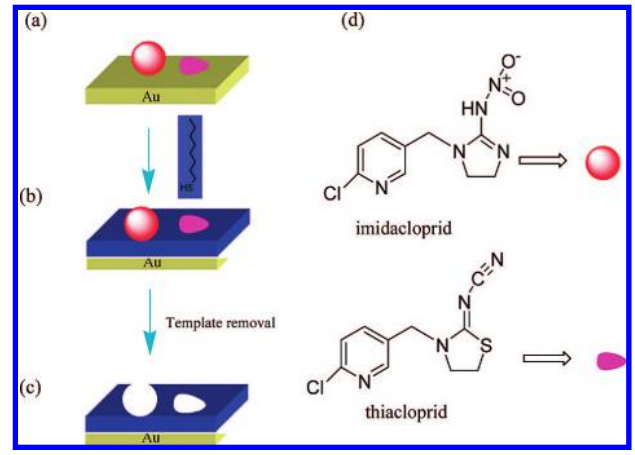

Figure 1. Schematic illustration of neonicotinoid-selective surface binding sites created by using 2D molecular imprinting techniques. (a) Templates (thiacloprid and imidacloprid) were preadsorbed on a gold surface. (b) Alkanethiols self-assembled around the preadsorbed templates. (c) The templates were removed from the surface and two different molecularly imprinted binding sites were created. (d) Molecular structures of imidacloprid and thiacloprid.

to detect imidacloprid and thiacloprid simultaneously by using a single QCM unit, a two-template-imprinted method was developed.[40] Unlike traditional MIMs prepared from one template, we employed two templates (imidacloprid and thiacloprid) during the molecular imprinting procedure. Thus, the MIM prepared using this new method permits the detection of both imidacloprid and thiacloprid (Figure 1).

EXPERIMENTAL SECTION

Chemicals. Imidacloprid, thiacloprid, octanethiol, and hexadecanethiol were purchased from Sigma Aldrich (Singapore). All solvents used in this study were HPLC grade. Water was purified by using a Milli-Q system (Millipore, U.S.A.). The celery juice was prepared from fresh celery (neonicotinoids-free) by using a blender. After centrifuging several times (to remove suspended solids), neonicotinoids were dissolved in the clear celery juice to obtain the desired concentrations.

Preparation of Molecularly Imprinted Monolayers. Gold QCM sensor chips (9 MHz, bare-gold, ANT technology, Taiwan) were first immersed overnight in ethanolic solutions containing either 5 mM thiacloprid or 5 mM imidacloprid to allow the adsorption of thiacloprid or imidacloprid onto the gold surfaces. Increases in surface ellipsometric thicknesses (6 ± 3 Å for thiacloprid and 4 ± 2 Å for imidacloprid, respectively) suggest that thiacloprid and imidacloprid adsorbed on the surfaces after the immersion. After rinsing with deionized water, gold sensor chips were placed on top of a vial containing 200 mg of octanethiol or hexadecanethiol. Because of the low volatility of these thiols, the vial was kept in a desiccator connected to a vacuum pump. Vacuum (~16 mbar) was applied for 10 min to fill the desiccator with thiol vapor. Finally, the surface was rinsed thoroughly with pure ethanol and deionized water sequentially to remove thiacloprid or imidacloprid and blown dry with nitrogen.

Ellipsometry. Ellipsometric thicknesses of SAMs on gold surfaces (average reflective index $n = 0.29$, $k = -3.4456$) were

(25) Karousos, N. G.; Aouabdi, S.; Way, A. S.; Reddy, S. M. *Anal. Chim. Acta* **2002**, *469*, 189–196.
(26) Ye, L.; Haupt, K. *Anal. Bioanal. Chem.* **2004**, *378*, 1887–1897.
(27) Haupt, K.; Noworyta, K.; Kutner, W. *Anal. Commun.* **1999**, *36*, 391–393.
(28) Lieberzeit, P. A.; Schirk, C.; Glanznig, G.; Gazda-Miarecka, S.; Bindeus, R.; Nannen, H.; Kauling, J.; Dickert, F. L. *Superlattices Microstruct.* **2004**, *36*, 133–142.
(29) Stanley, S.; Percival, C. J.; Auer, M.; Braithwaite, A.; Newton, M. I.; McHale, G.; Hayes, W. *Anal. Chem.* **2003**, *75*, 1573–1577.
(30) Panasyuk-Delaney, T.; Mirsky, V. M.; Ulbricht, M.; Wolfbeis, O. S. *Anal. Chim. Acta* **2001**, *435*, 157–162.
(31) Panasyuk-Delaney, T.; Mirsky, V. M.; Piletsky, S. A.; Wolfbeis, O. S. *Anal. Chem.* **1999**, *71*, 4609–4613.
(32) Lieberzeit, P. A.; Gazda-Miarecka, S.; Halikias, K.; Schirk, C.; Kauling, J.; Dickert, F. L. *Sens. Actuators B* **2005**, *111*, 259–263.
(33) Mirsky, V. M.; Hirsch, T.; Piletsky, S. A.; Wolfbeis, O. S. *Angew. Chem., Int. Ed.* **1999**, *38*, 1108–1110.
(34) Chidsey, C. E. D.; Bertozzi, C. R.; Putvinski, T. M.; Mujsce, A. M. *J. Am. Chem. Soc.* **1990**, *112*, 4301–4306.
(35) Chailapakul, O.; Crooks, R. M. *Langmuir* **1993**, *9*, 884–888.
(36) Liu, J.; Shin, Y.; Nie, Z.; Chang, J. H.; Wang, L. Q.; Fryxell, G. E.; Samuels, W. D.; Exarhos, G. J. *J. Phys. Chem. A* **2000**, *104*, 8328–8339.
(37) Li, X.; Husson, S. M. *Biosens. Bioelectron.* **2006**, *22*, 336–348.
(38) Wei, X.; Li, X.; Husson, S. M. *Biomacromolecules* **2005**, *6*, 1113–1121.
(39) Li, X.; Husson, S. M. *Langmuir* **2006**, *22*, 9658–9663.
(40) Dickert, F. L.; Achatz, P.; Halikias, K. *Fresenius J. Anal. Chem* **2001**, *371*, 11–15.

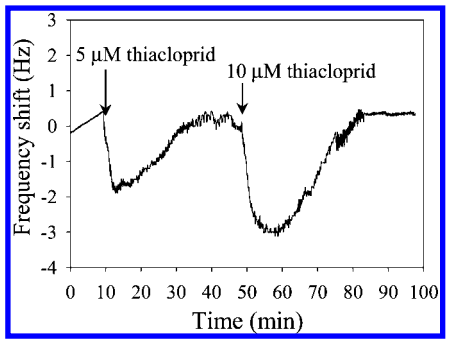

Figure 2. Changes in QCM frequency in response to the injection of 5 and 10 μM thiacloprid, respectively. The arrow indicates the time when the solution starts to flow over the sensor chip, not the injection time.

measured by using a Stokes Ellipsometer LSE (Gaertner, U.S.A.) at a wavelength of 632 nm and a fixed angle of 70°. The ellipsometric thicknesses were calculated by assuming a single reflective index of 1.46 and a one-layer model. Each thickness represents an average thickness of five different spots.

Quartz Crystal Microbalance (QCM). All QCM experiments were performed by using an affinity detection system (resolution = 0.1 Hz) manufactured by ANT technology (Taipei, Taiwan). For each measurement, 300 μL of sample solution was injected into a sample loop (volume = 100 μL) and then delivered to a molecularly imprinted sensor chip by using a peristaltic pump. Teflon tubings with an internal diameter of 0.5 mm were used to connect each component of the system. Deionized water was used as a running buffer, and the flow rate was fixed at 30 μL/min. Under this flow rate, it takes 200 s for the sample solution to reach the QCM sensing unit. Used QCM chips were cleaned by immersing in 10 μL dichromate acid for 15 min and then rinsed thoroughly with copious amounts of deionized water.[41]

RESULTS AND DISCUSSION

On-Line Monitoring of Thiacloprid. First, we prepared a thiacloprid-imprinted sensor chip and used it to detect thiacloprid and imidacloprid in aqueous solutions. As shown in Figure 2, when 5 μM of thiacloprid was injected, the frequency decreased by 2.1 Hz after 200 s. This result suggests that the binding of thiacloprid molecules to the thiacloprid-imprinted surface is a fast process. However, in the next 20 min, the frequency gradually went back to its original value, indicating that the binding of thiacloprid to the sensitive layer is reversible. Similarly, when 10 μM of thiacloprid was injected into the system, the frequency decreased by 3.0 Hz in 200 s and went back to its original value after 25 min. In contrast, the injection of 10 μM imidacloprid solution only caused 0.4 Hz decrease in the frequency. These results suggest that the thiacloprid-imprinted surface can recognize thiacloprid with good specificity in a real-time manner. The high specificity is probably due to the rigid chloropyridinyl structures of thiacloprid and imidacloprid.[42,43] When they adsorb on a gold surface and lay flat, their unique molecular structures determine the shapes of the 2D cavities formed among the SAMs of organothiols.

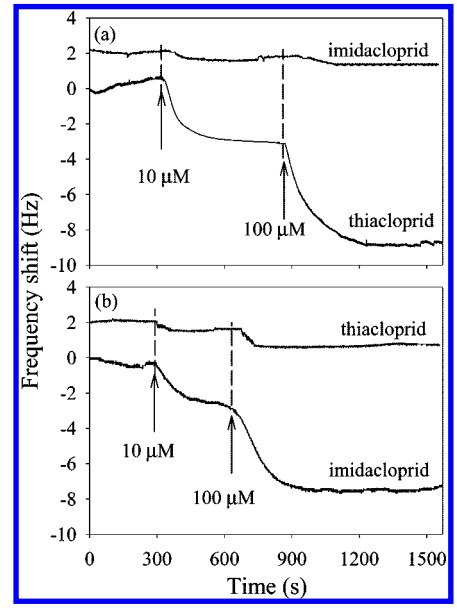

Figure 3. Responses of QCM frequency to multiple injections of imidacloprid or thiacloprid (with increasing concentrations) onto (a) a thiacloprid-imprinted surface and (b) an imidacloprid-imprinted surface, which were prepared by the self-assembly of octanethiol around the preadsorbed thiacloprid and imidacloprid, respectively.

Thus, the cavity formed by using thiacloprid as a template only matches the shape of thiacloprid such that it cannot bind imidacloprid tightly.

Equilibrium Model. To investigate the binding behaviors of thiacloprid and imidacloprid further, various concentrations of thiacloprid and imidacloprid were injected sequentially as shown Figure 3a. The change in QCM frequency, ΔF (Hz), after the equilibrium can be converted to an increase in surface mass, Δm (g) through the Kanazawa−Gordon equation.[44−46]

$$\Delta F = -\frac{2F_R^2 \Delta m}{A\sqrt{\rho_q \mu_q}} - F_R^{3/2}\sqrt{\frac{\Delta\rho\Delta\eta}{\pi\rho_q\mu_q}} \quad (1)$$

where F_R is resonant frequency of the quartz crystal (9×10^6 Hz), ρ_q (2.65 g/cm^3) and μ_q (2.95×10^{11} dyne/cm^2) are the density and shear modulus of quartz, respectively. A is area of the gold electrode on the quartz crystal (0.10 cm^2), $\Delta\rho$ and $\Delta\eta$ are the changes in solution density and viscosity, respectively, because of the presence of thiacloprid. If we assume that both $\Delta\rho$ and $\Delta\eta$ are small, the second term is negligible, and eq 1 can be simplified to a Sauerbrey equation. In that case, a decrease of 1 Hz in ΔF corresponds to an increase of 5.5 ng/cm^2 in surface mass density ($\Delta m/A$). The relationship between $\Delta m/A$ and thiacloprid concentration in the bulk, C, is shown in Table 1. These data can be modeled by using the Langmuir adsorption isotherm

$$\frac{\Delta m/A}{\Delta m_{max}/A} = \frac{C}{C + K_d} \quad (2)$$

where $\Delta m_{max}/A$ is the maximum mass density and K_d is the

(41) Su, X.; Chew, F. T.; Li, S. F. Y. *Appl. Sci.* **2000**, *16*, 107–114.
(42) Tomizawa, M.; Talley, T. T.; Maltby, D.; Durkin, K. A.; Medzihradszky, K. F.; Burlingame, A. L.; Taylor, P.; Casida, J. E. *Proc. Natl. Acad. Sci. U.S.A.* **2007**, *104*, 9075–9080.
(43) Nakayama, A.; Sukekawa, M.; Eguchi, Y. *Pestic. Sci.* **1997**, *51*, 157–164.
(44) Kanazawa, K. K.; Gordon, J. G., II *Anal. Chem.* **1985**, *57*, 1171–1172.
(45) Rickert, J.; Brecht, A.; Gopel, W. *Anal. Chem.* **1997**, *69*, 1441–1448.
(46) Sauerbrey, G. *Z. Phys.* **1959**, *155*, 206–222.

Table 1. Changes in QCM Frequency ΔF (Hz) Induced by Adsorption of Imidacloprid and Thiacloprid on 2D MIMs

	thiacloprid-imprinted[a]				imidacloprid-imprinted			
	thiacloprid		imidacloprid		thiacloprid		imidacloprid	
C (μM)	ΔF	$\Delta m/A$[b]	ΔF	$\Delta m/A$	ΔF	$\Delta m/A$	ΔF	$\Delta m/A$
1	−0.56	3.07	−0.10	0.55	−0.20	1.10	−0.55	3.03
5	−2.56	14.11	−0.20	1.09	−0.41	2.24	−2.20	12.09
10	−3.18	17.47	−0.40	2.20	−0.50	2.75	−3.02	16.59
40	−4.05	22.28	−0.73	3.99	−0.76	4.17	−3.85	21.15
100	−6.10	33.55	−0.80	4.40	−0.90	4.95	−4.36	23.99
K_d[c]	11.19		23.12		9.22		8.67	
$\Delta m_{max}/A$[d]	37.74		6.35		5.27		29.48	

[a] The sensitive layer on the QCM sensor chip was formed from octanethiol. [b] The surface mass density $\Delta m/A$ (ng/cm^2) was obtained from eq 1. [c] Dissociation constant K_d (μM) was obtained from eq 2 by using a least-squares fitting method. [d] The maximum mass density $\Delta m_{max}/A$ (ng/cm^2) was obtained from eq 2 by using a least-squares fitting method.

dissociation constant. Both parameters shown in Table 1 were obtained by using least-squares fitting methods. We can draw two principal conclusions from Table 1. First, on a thiacloprid-imprinted surface, $\Delta m/A$ caused by the binding of thiacloprid is higher than that of imidacloprid, suggesting that the thiacloprid-imprinted surface has higher selectivity for thiacloprid. Second, on the thiacloprid-imprinted surface, the K_d value for thiacloprid (11.19 μM) is smaller than the one for imidacloprid (23.12 μM). The smaller K_d value for thiacloprid is consistent with the high selectivity for thiacloprid on the thiacloprid-imprinted surface. Next, we injected both thiacloprid and imidacloprid solutions onto an imidacloprid-imprinted surface. Increases in mass density because of the adsorption of imidacloprid and thiacloprid were also shown in Table 1. Notably, imidacloprid-imprinted surface binds selectively to imidacloprid over thiacloprid. These results, when combined, suggest that the selectivity for thiacloprid and imidacloprid can be obtained by using either thiacloprid- or imidacloprid-imprinted monolayers.

Kinetic Models. The increase in surface mass density because of the binding of thiacloprid onto a thiacloprid-imprinted surface at time t can be described as

$$\frac{d\Delta m/A}{dt} = k_{on}C(\Delta m_{\infty}/A - \Delta m/A) - k_{off}\Delta m/A \qquad (3)$$

where k_{on} and k_{off} are the association and dissociation rate constants, respectively. $\Delta m_{\infty}/A$ is the increase in surface density when all surface adsorption sites are occupied (i.e., $\Delta m_{\infty}/A = \Delta m_{max}/A$ when $C \rightarrow \infty$). Solving eq 3 gives

$$\frac{\Delta m}{A} = \frac{\Delta m_{max}}{A}(1 - e^{-t/\tau}) \qquad (4)$$

where τ is the characteristic time ($\tau^{-1} = k_{on}C + k_{off}$). Figure 4a shows a linear relationship between τ^{-1} and C. Therefore, k_{on} and k_{off} can be calculated from the slope and intercept of the best-fitting line in Figure 4a, and their values are listed in Table 2. It is noted that the k_{off}/k_{on} ratio is 13.11 μM, which is fairly consistent with the K_d value obtained from our equilibrium

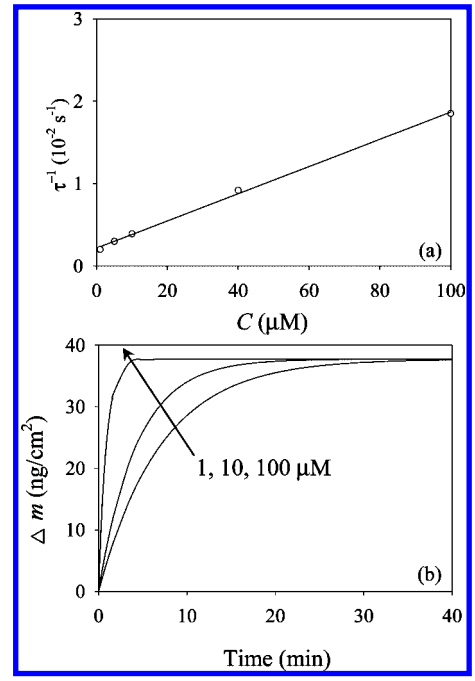

Figure 4. (a) Linear relationship between the reciprocal of the characteristic time (τ^{-1}) and the thiacloprid concentration in the bulk. (b) Predicted kinetic curves for different thiacloprid concentrations (1, 10, and 100 μM) based on the kinetic parameters obtained in part A.

Table 2. Kinetic Parameters for the Adsorption of Thiacloprid and Imidacloprid onto 2D MIMs

analytes	thiols	$k_{on} \times 10^3$ (μM^{-1}s^{-1})	$k_{off} \times 10^3$ (s^{-1})	k_{off}/k_{on} (μM)	K_d (μM)
		Thiacloprid-Imprinted			
thiacloprid	hexadecanethiol	0. 439	1.19	2.71	2.37
thiacloprid	octanethiol	0.167	2.19	13.11	11.19
imidacloprid	octanethiol	0.156	4.09	26.17	23.12
		Imidacloprid-Imprinted			
imidacloprid	hexadecanethiol	0.325	1.36	4.18	3.65
imidacloprid	octanethiol	0.194	2.03	10.42	8.67
thiacloprid	octanethiol	0.172	2.08	12.08	9.22

model (Table 2). Moreover, theoretical binding curves based on k_{on} and k_{off} at different thiacloprid concentrations are shown in Figure 4b. The binding curves suggest that if the concentration of thiacloprid is 100 μM, 98% of the thiacloprid binding sites will be occupied by thiacloprid after 200 s. Kinetic parameters for the binding of imidacloprid onto the imidacloprid-imprinted surface were also obtained following a similar procedure and are summarized in Table 2.

Effect of MIM thickness. In an effort to lower the detection limit, we compared MIMs formed from octanethiol and hexadecanethiol. First, we characterized MIMs formed from octanethiol and hexadecanethiol (both were thiacloprid-imprinted) with ellipsometry, and their thicknesses were found to be 3 ± 1 Å and 8 ± 1 Å, respectively. However, because the theoretical molecular length of the latter is 100% longer than the former, we can estimate that the surface coverage on both surfaces is similar. Therefore, the numbers of binding sites on both surfaces are comparable. Next, we obtained K_d for these two MIMs by using QCM. It was found that the thiacloprid-imprinted MIM prepared from hexadecanethiol has a K_d of 2.37 μM for thiacloprid, which is

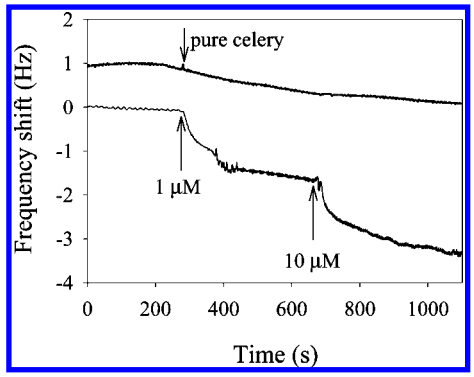

Figure 5. Responses of QCM frequency to multiple injections of thiacloprid in celery matrix onto the thiacloprid-imprinted sensor chip. MIMs were prepared by the self-assembly of hexadecanethiol around the preadsorbed thiacloprid template.

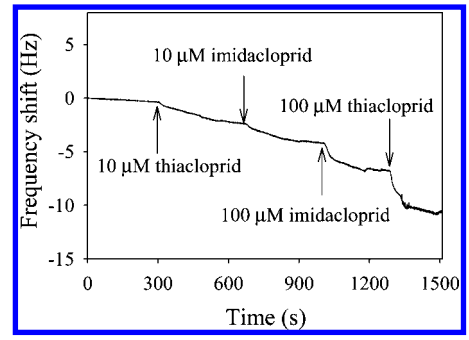

Figure 6. Responses of QCM frequency to multiple injections of thiacloprid or imidacloprid in celery juice onto the molecular imprinting sensor chip. MIMs were prepared by the self-assembly of hexadecanethiol around the preadsorbed thiacloprid and imidacloprid (two templates).

5 times smaller than the K_d (11.19 μM) obtained from the MIM prepared from octanethiol. This result suggests that the MIM formed from hexadecanethiol binds stronger to thiacloprid than that formed from octanethiol. One possible reason is that the longer alkyl chain from hexadecanethiol may stabilize molecules adsorbed on the surface or prevent them from escaping from the binding sites. Similarly, K_d of imidacloprid onto the imidacloprid-imprinted surface decreased two-fold when we used hexadecanethiol to prepare MIMs. In the following experiments, we used hexadecanethiol to prepare MIMs since they offer a better detection limit.

Matrix Effects. To demonstrate that neonicotinoids in vegetables can also be detected by using this method, we prepared celery juice as a vegetable matrix and spiked it with different concentrations of thiacloprid. First, we exposed a thiacloprid-imprinted QCM sensor chip to pure celery juice. After 15 min, the frequency only decreased 1.0 Hz, which suggests that most ingredients in celery juice do not adsorb nonspecifically on the MIM-coated QCM surface. This result is surprising because Husson and Li showed that nonspecific adsorption is significant on the MIM formed from 2-mercaptoethanol.[39] There are two possible explanations for the low nonspecific adsorption observed in our study. First, the flow rate in our QCM system is high enough (30 μL/min) such that nonspecifically adsorbed celery ingredients were washed away. Second, ingredients in celery juice are very hydrophilic such that they do not adsorb on hydrocarbon-terminated surfaces. Next, we injected celery juice containing 1 μM of thiacloprid onto a thiacloprid-imprinted QCM sensor chip. This concentration is equivalent to 0.25 mg of thiacloprid per kilogram of celery juice. As shown in Figure 5, the frequency decreased by 1.5 Hz ($\Delta m/A = 8.25$ ng/cm^2). This detection limit is lower than the maximum allowable thiacloprid residues for some fruiting vegetables set by the EU (0.5 to 1 mg/kg). Moreover, if the concentration of thiacloprid was increased to 10 μM, then the frequency decreased by another 3.9 Hz ($\Delta m/A = 21.45$ ng/cm^2), which is only 7.5% more than the $\Delta m/A$ measured in water. These results suggest that the celery juice does not cause any significant interference in the detection method. Thiacloprid still can bind to the thiacloprid-imprinted surface even in the presence of celery juice, and the detection limit is similar to that in water.

Two-Template-Imprinted Surfaces. In some applications, sensors which can respond to both thiacloprid and imidacloprid are needed. Although this can be achieved by using two QCM sensors in series, one for thiacloprid and the other for imidacloprid, a single QCM sensor which can respond to both thiacloprid and imidacloprid is more ideal. To achieve this goal, we created a MIM on a QCM sensor chip by using two templates (thiacloprid and imidacloprid) together. Figure 6 shows responses of the QCM to multiple injections of celery juice containing thiacloprid and imidacloprid, respectively. When we injected 10 μM of thiacloprid, the frequency of the QCM decreased by 2.0 Hz ($\Delta m/A = 11.00$ ng/cm^2). Apparently, the increase in mass density is lower than that in Figure 5. This can be explained by the decrease in surface density of thiacloprid-imprinted sites because of the presence of two templates during the imprinting procedure. Subsequently, we injected celery juice containing 10 μM of imidacloprid, and the frequency decreased by another 1.8 Hz. When we further increased the concentrations of imidacloprid and thiacloprid to 100 μM, the frequency decreased further by another 2.8 and 3.8 Hz, respectively. These results, when combined, suggest that we can detect two neonicotinoids in aqueous solutions or vegetable juices simultaneously with the two-template-imprinted technique.

CONCLUSIONS

In this study, we have successfully demonstrated the application of QCM sensors decorated with 2D MIMs for identification and quantification of thiacloprid and imidacloprid in a real-time manner. We also studied the binding of neonicotinoids onto the MIMs by using alkanethiols with different chain lengths. Our results show that the dissociation constant of thiacloprid on a thiacloprid-imprinted MIM prepared from hexadecanethiol is 2−5 times smaller than the one prepared from octanethiol. Furthermore, we found that celery juice caused minimal interferences ($\Delta m/A$ only increases by 7.5% compared to the experiments performed in water), which allows us to obtain a detection limit (0.25 mg/kg) that is lower than the EU standard for fruiting vegetables. Finally, we developed a two-template-imprinted method and used it for the simultaneous detection of thiacloprid and imidacloprid. This principle for developing 2D molecular imprinted QCM sensor may have potential utility in the on-line monitoring

of neonicotinoids in water samples or in the detection of various neonicotinoids residues found in fruits and vegetables.

ACKNOWLEDGMENT

This work was supported by the Ministry of Education's AcRF Tier 1 under Grant RG-279-001-036 and Agency for Science, Technology and Research (A*STAR) under Grant 0521010099 in Singapore.

Received for review August 26, 2008. Accepted November 5, 2008.

AC801786A